論文 80-17-3-4

System Resolution Recovery by Motion Blur Recovery Technique-- Particular Application to X-ray Computerized Tomography (移動Blur 回復法을 이용한 分解能 向上—X-ray C. T.에의 應用)

李 秀 榮*, 金 洪 錫**

(Lee, Soo Young and Kim Hong Suk)

要 約

모든 디지탈 影像界에서 검출기는 일정한 크기를 가지며, 이에 의해 影像은 흐려지고 空間分解能은 저하된다. 이제까지는 검출기 크기를 줄임으로써, 즉 검출기 수효를 증가시킴으로써 이 問題를 解決해 왔다. 本論文에서는 光學에서 사용한 방법에 의한 空間分解能 向上을 空間 및 周波數 帶域에서 시도하였다. 또한 이 방법을 CT(電算化 斷層 映像 處理機)에 應用하였으며 검출기 수효를 증가하지 않고서도 空間分解能이 매우 向上됨을 알 수 있었다. 이 방법에 대한 基本理論 및 simulation 結果를 整理하였다.

Abstract

The degradation of image due to the finite size of sensing devices has been one of the problems in all digital imaging systems. The basic study on the improvement of the spatial resolution was carried out in both spatial and frequency domains by the resolution recovery techniques which have been used in optics.

Here, the techniques were applied to CT (Computerized Tomography) system, and image with finer resolution was obtained by these techniques. The basic theory is described and the results of the simulation are shown.

I. Introduction

In analog imaging systems, the motion of an object or a camera causes "Blurring" to the image. The methods of the removal of this degradation have been studied by a number of investigators.[1, 2] This degradation of image due to the finite size of the sensing device is equivalent to motion blur, since both of them are caused by "integration" or "averaging" of the imaging object.[8, 9, 10]

To remove the effect of this motion blur or averaging of image, some image recovery techniques in digital form of interest is the image resolution recovery in CT system.[3, 4]

Since the first CT system was introduced, improvement of the spatial resolution has been attempted by increasing the number of detectors, i.e., decreasing the detector width since the detector size (width and length) determines the resolution (sampling as well as point or line spread fuction).

Such an approach, however, is costly and also the narrower the detector width becomes, the smaller the number of absorbed photons in one detector, and therefore it causes the reduction of the S/N ratio.

*準會員, **正會員, 韓國科學院 電氣 및 電子工學科
(Dept. of Electrical Science, KAIS)

接受日字 : 1979年 11月 2日

For that reason, it is not usually recommended to increase the number of detectors without considering the reduction of S/N ratio.

Another approach to improve the spatial resolution is finer sampling with fixed detector size and then recovery of the resolution. Even in the latter case, degradation of S/N ratio is the same, the advantage gained, however, is cost effectiveness, i.e., finer resolution can be obtained without increasing the number of detectors. This kind of approach, i.e., finer sampling with wide detector followed by the recovery of resolution by decovolution technique can be applied to both XCT (X-ray CT) as well as ECT (Emission CT).[4, 5]

II. Basic Theory

The ideal projection data is illustrated in Fig. 1-(a). When we use only 4 detectors with width T, the projection data obtained is degraded as shown in Fig. 1-(b), where the fine details are integrated within the each detector. And if the width of detector is decreased to T/4, the resolution improved projection data is obtained as shown in Fig. 1-(c).

Now let's observe the overlap-sampled data which is sample 4 times denser with same size of detectors (see Fig. 1-(d)). In this case, the projection data obtained contain the informations of the differences ($g_{i+i} - g_i$). This suggests the possibility of improving the spatial resolution.

The schematic representation of degradation is given in Fig. 2, where degraded image g(x) and degraded image with added noise $g_o(x)$ are given as

$$g = f * h$$
$$g_o = g + n$$

Here, we would like to extract f from g_o in the presence of noise n.

If the motion of detectors between successive samplings is considered (continuous motion assumed), the degradation function h can be modeled as a form shown in Fig. 3-(a), where D is the sampling interval. This degradation function, however, is assumed to be a shape as shown in Fig. 3-(b) for simplicity in spatial domain processing.

For the recovery of the resolution to the

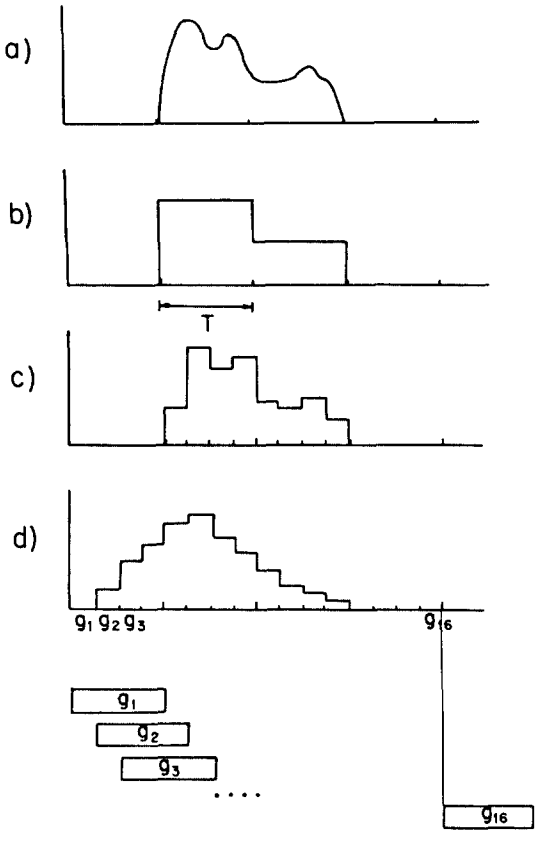

Fig. 1. The effect of finite size of sensor to the image.
a) Original image
b) The image sampled by 4 detectors of width T
c) The image sampled by 16 detectors of width T/4
d) 4 times overlap-sampled image by 4 detectors of width T

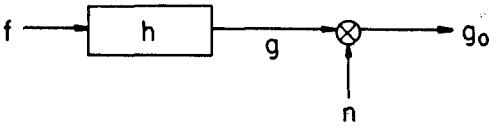

Fig. 2. The schematic representation for the blurring model.

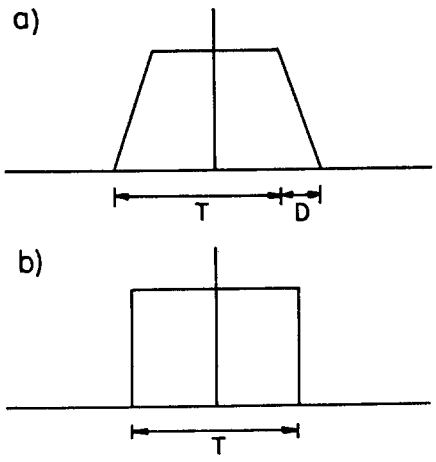

Fig. 3. Degradation functions.
a) Motion of detectors is considered
b) Motion of detectors is not considered

extent where the only limiting factor is sampling, following two approaches are suggested.

1. Differential Method of Spatial Domain

The one-dimensional projection data g(x) can be described as follows,

$$g(x) = 1/T \int_{x-T/2}^{x+T/2} f(y)\,dy \qquad (1\text{-}1)$$

By differentiating both sides with respect to x, we obtain,

$$f(x) = f(x-T) + T \cdot g'(x-T/2) \qquad (1\text{-}2)$$

Restoring a sharp image by analogue circuits was successful.[8, 9, 10] In our case, x is not continuous but discrete.

That is,

$$f(k \cdot \Delta x) = f(k \cdot \Delta x - T) + T \cdot g'(k \cdot \Delta x - T/2) \qquad (1\text{-}3)$$

where k = 1, 2, 3, ...
And if we set Nd = T/Δx, Eq. (1-3) can be written as,

$$f(k) = f(k-N_d) + T \cdot g'(k-k_d)$$

$$= f(k-N_d) + T \cdot (g(k-k_d) - g(k-k_d-1)) \qquad (1\text{-}4)$$

where k_d has to be determined as an initial condition so that $g(k-k_d)$ becomes the first projection data that includes f(k).

For example, in the case that we sample the projection data as shown in Fig. 1-(d), the value of k_d is 3. From Eq.(1-4), one can see that if initial values of $f(k-N_d)$ ($k = 1, 2, \ldots N_d$) are known, f(k) can be calculated. That is, if we know $f(1), f(2), \ldots . f(N_d)$, we can obtain the rest of f(k) from the projection data g(k) as follows,

$$f(N_d+1) = f(1) + T \cdot (g(N_d+1-k_d) - g(N_d-k_d))$$

$$f(N_d+2) = f(2) + T \cdot (g(N_d+2-k_d) - g(N_d+1-k_d)) \qquad (1\text{-}5)$$

$$f(2N_d) = f(N_d) + T \cdot (g(2N_d-k_d) - g(2N_d-1-k_d))$$

$$f(2N_d+1) = f(N_d+1) + T \cdot (g(2N_d+1-k_d) - g(2N_d-k_d))$$

In the CT system, we can let the initial values be known values to start the evaluation process. In reality, noise is added and Eq.(1-4) becomes,

$$f(k) = f(k-N_d) + T \cdot (g_o(k-k_d) - g_o(k-k_d-1)) \qquad (1\text{-}6)$$

The resolution recovery technique given in Eq. (1-5) is simple and easy to implement, however, it suffers from noise. Differential method of Eq.(1-6) is sensitive even to the small noise and generates quite large error in cluculating f(k). Since this differential method is sequential, the noise propagates and accumulates (see Appendix).

2. Wiener Filter Method in Frequency Domain

From Fig. 2, and Fig. 3, the blurred $G(\omega)$ can be rewritten, as,

$$G(\omega) = H(\omega) \cdot F(\omega) \qquad (2\text{-}1)$$

where

$G(\omega) = \mathcal{F}(g(x))$

$F(\omega) = \mathcal{F}(f(x))$

$H(\omega) = \mathcal{F}(h(x))$

This indicates recovery of original image $F(\omega)$ by simple inverse filter, i.e.,

$$F(\omega) = G(\omega)/H(\omega)$$
$$= H_1(\omega) \cdot G(\omega) \qquad (2\text{-}2)$$

where $H_1(\omega) = 1/H(\omega)$

But in many cases, $H_1(\omega)$ has poles and diverges at these poles. In addition, $H_1(\omega)$ increases at high frequency region and hence noise is enhanced.

To overcome these difficulties, "Wiener filter" or "Least square filter" approach can be chosen. As we know, the Wiener filter can be modified[5, 6] as,

$$H_W(\omega) = H^*(\omega)/(|H(\omega)|^2 + \Gamma) \qquad (2\text{-}3)$$

where Γ is the noise to signal power density ratio and assumed to be a constant, and * means complex conjugate.

Rewriting Eq.(2-2), the recovered image $F(\omega)$ is,

$$F(\omega) = H_W(\omega) \cdot G_O(\omega) \qquad (2\text{-}4)$$

where $G_O(\omega) = \mathcal{F}(g_O(x))$

Once $F(\omega)$ is obtained, we can get the resolution-improved projection data $f(x)$ (or image) simply by taking inverse Fourier transform, which removes the problem arising from the poles of $H_1(\omega)$. If the motion of detectors is considered, the transfer function is as shown in Fig. 2-(a) and is,

$$h(x) = \begin{cases} (x+D_2)/(D\cdot T) & -D_2 \leqslant x \leqslant -D_1 \\ 1/T & -D_1 \leqslant x \leqslant D_1 \\ -(x-D_2)/(D\cdot T) & D_1 \leqslant x \leqslant D_2 \\ 0 & \text{otherwise} \end{cases} \qquad (2\text{-}5)$$

where $D_1 = (T-D)/2$, $D_2 = (T+D)/2$.

$H(\omega)$ is then,

$$H(\omega) = \int_{-D_1}^{D_1} (1/T)\, e^{-j\omega x}\, dx + \int_{-D_2}^{-D_1} (x+D_2)/(D\cdot T)\, e^{-j\omega x}\, dx - \int_{D_1}^{D_2} (x-D_2)/(D\cdot T)\, e^{-j\omega x}\, dx$$
$$= 2(\cos\omega D_1 - \cos\omega D_2)/(\omega^2 D\cdot T) \qquad (2\text{-}6)$$

And if the motion of detectors can be neglected, the transfer function becomes,

$$H(\omega) = 1/T \int_{-T/2}^{T/2} e^{-j\omega x}\, dx$$
$$= 2\cdot\sin(\omega T/2)/(\omega\cdot T) \qquad (2\text{-}7)$$

III. Simulation and Results

1. "Integration Blur (Linear Motion)" Recovery

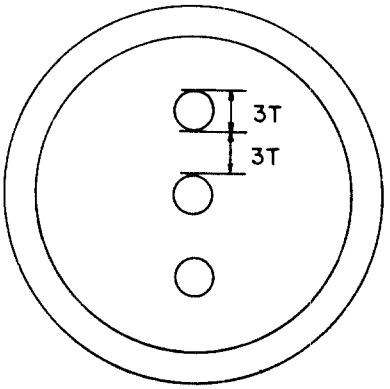

Fig. 4. Test phantom for motion blur recovery.

To test the above two resolution recovery methods, we carried out simulation with a phantom shown in Fig. 4.

The gray level of the ring and small circles is 30 with zero background. Original picture is blurred with 5-times of sampling width. The noise is assumed Gaussian and signal-independent. The two recovery techniques, mentioned previously, were tried at various noise levels and the results were shown in Fig. 8, 9, 10, and 11. The dimension of image was 64 x 64.

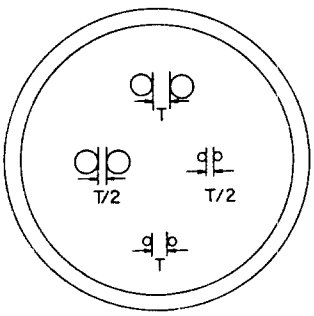

Fig. 5. Test phantom for parallel system T is a detector width.

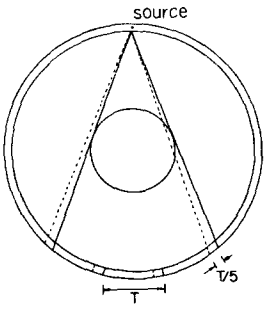

Fig. 6. Application to stationary ring system T is a detector width.

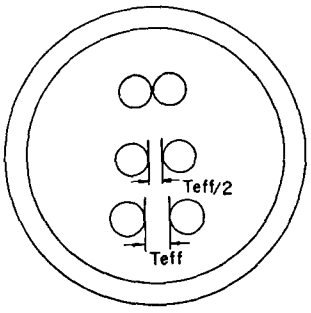

Fig. 7. Test phantom for stationary ring system T_{eff} is a effective width of detector.

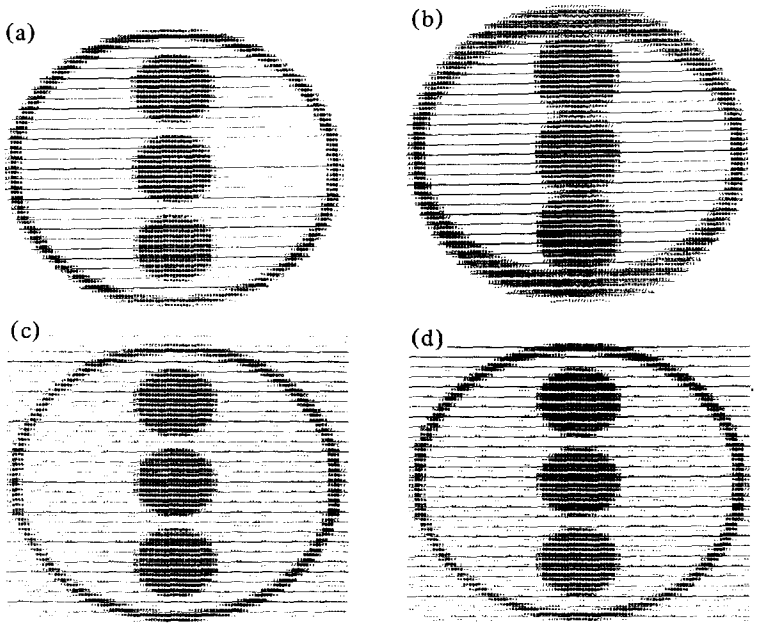

Fig. 8. Motion Blur Recovery for noise level of 0.3%.
a) Image with noise.
b) Blurred image with noise.
c) Recovered image by Wiener filter method.
d) Recovered image by differential method.

The differential method propagates noise as was expected, and could not be applied at 17% of noise while the Wiener filter approach allowed noise levels of up to 33% of signal level.

2. Application to CT System

A. Parallel system

In this simulation, we sampled projection data as shown in Fig. 1-(d). 80-views through 180° were taken and the motion of detectors was considered in the recovering process (Eq. (2-6)). The number of detectors was 32, and number of samplings was 128, i.e., sampling interval D is one quarter of the detector width T. The added noise is Gaussian and signal-dependent. The standard model of the phantom is shown in Fig. 6.

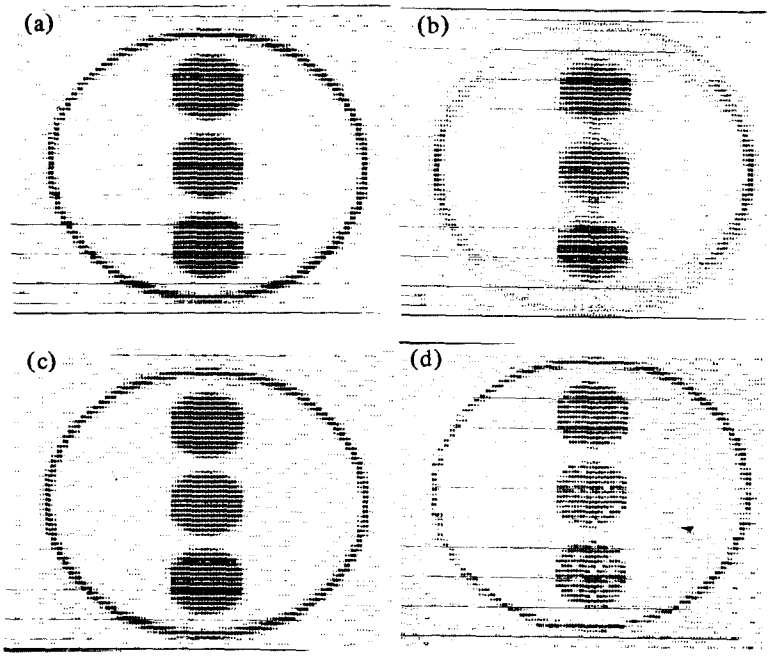

Fig. 9. Motion Blur Recovery for noise level of 3.3%.

a) Image with noise.
b) Blurred image with noise.
c) Recovered image by Wiener filter method.
d) Recovered image by differential method.

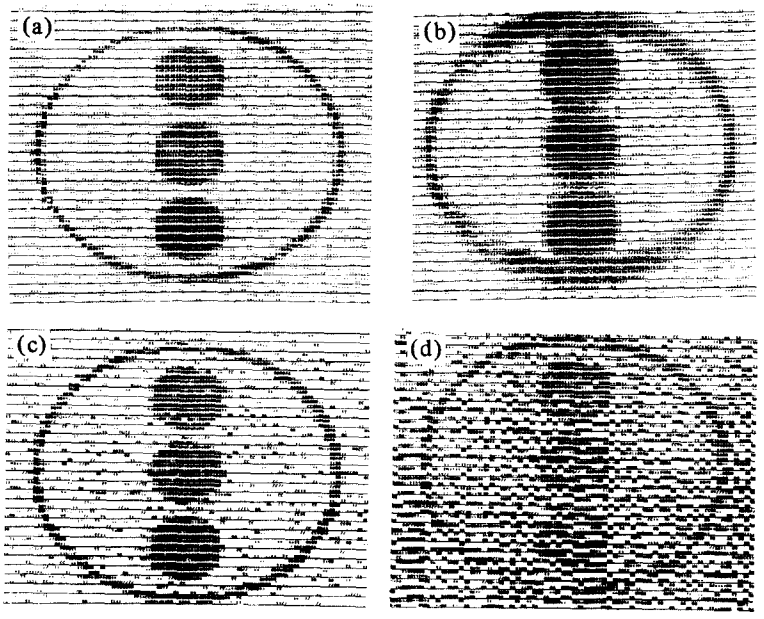

Fig. 10. Motion Blur Recovery for noise level of 17%.

a) Image with noise.
b) Blurred image with noise.
c) Recovered image by Wiener filter method
d) Recovered image by differential method.

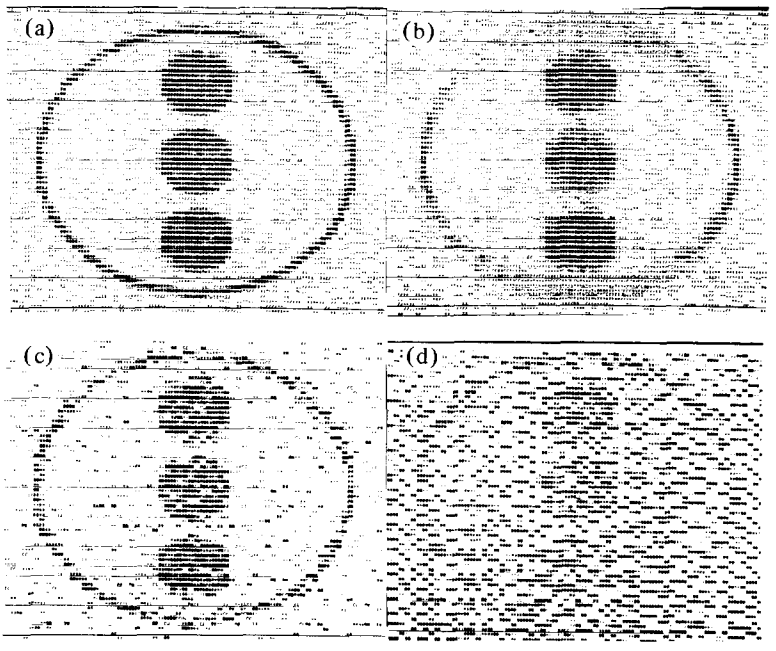

Fig. 11. Motion Blur Recovery for noise level of 33%.

a) Image with noise.
b) Blurred image with noise.
c) Recovered image by Wiener filter method.
d) Recovered image by differential method.

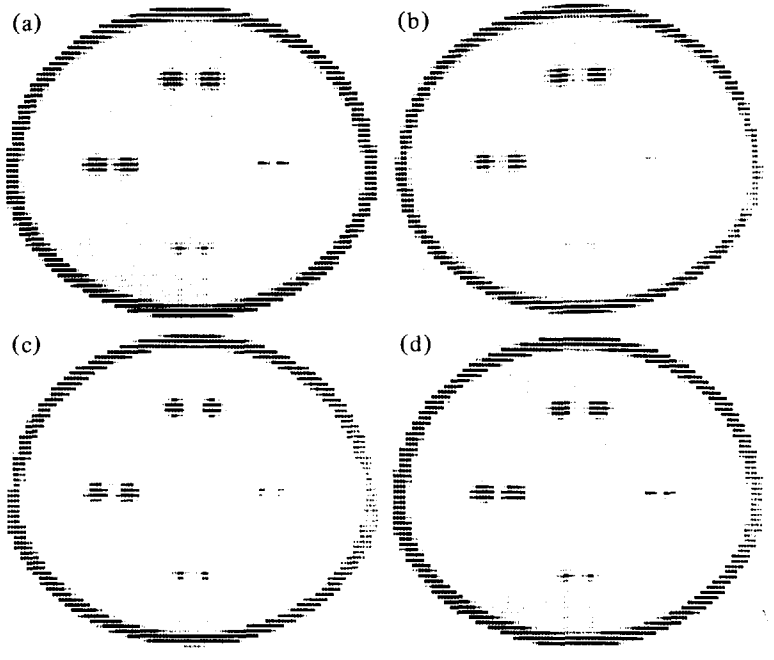

Fig. 12. Reconstructed image (64 x 64) for Parallel system with no-noise.

a) Image with 128 detectors for comparison.
b) Image with 32 detectors, not recovered.
c) Recovered image by differential method.
d) Recovered image by Wiener filter ($\Gamma=10^{-8}$).

The gray level of eight small circles was 95, and that of the outer ring was 100 with background of 70. Radius of the larger circle was T and that of the smaller one was T/2. For comparison, the simulation was carried out for the case where detector width is reduced to T/4, i.e., the number of detectors is 128 (in this case, noise level is doubled). In Fig. 12 and Fig. 13, the results of simulation are shown.

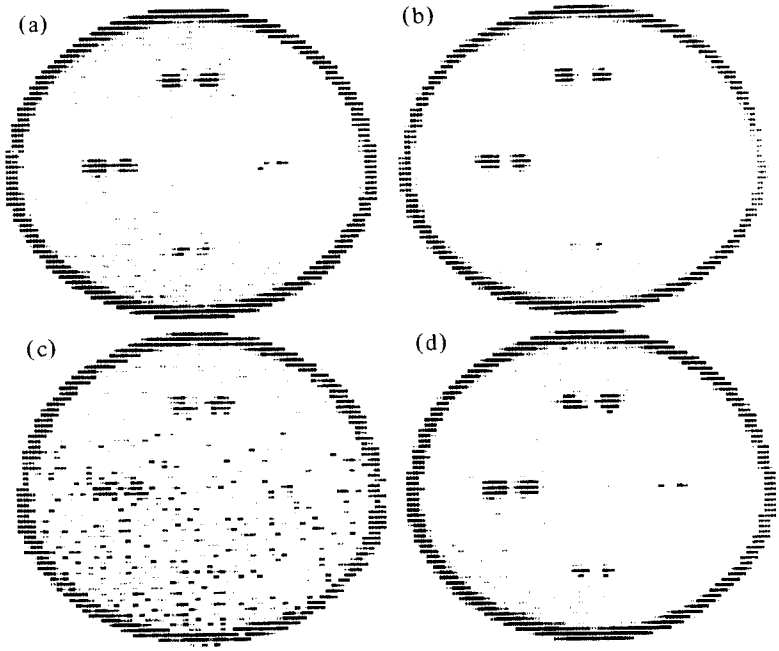

Fig. 13. Reconstructed image (64 x 64) for Parallel system.

a) Image with 128 detectors for comparison (0.8% noise).
b) Image with 32 detectors, not recovered (0.4% noise).
c) Recovered image by differential method (0.1% noise).
d) Recovered image by Wiener filter (0.4% noise, $\Gamma = 0.0002$).

As can be seen, when no noise is added, there are no significant differences among (b), (c), and (d) in Fig. 12. The differential method gives noisy image even with 0.1% of noise while Wiener filter approach allows as much as 0.4% of noise.

B. Resolution recovery applied to the stationary ring system with finite width detector array

Though the sampling is unlimited, in the stationary ring system, the spatial resolution is limited because of the finite detector width. If the detector array rotates by angle which corresponds to a certain fraction of the detector width (as an example, 1/5 of detector width at one time as shown in Fig. 6), we can improve the spatial resolution from the over-lap sampled data, similar to the previous parallel scanning case.

By rotating the detector array by one half the angle of the detector width T, the effective size of detector is reduced to T/2, and because the fan beam diverges, the actual sampling distance at the center of object is reduced to T/4. In a similar fashion, effective detector width can further be reduced by T/4 and T/8, etc.

To demonstrate the resolution recovery by the $\Delta\theta$ angular rotation, a simulation was made with the phantom shown in Fig. 7. The gray level of outer ring was 20, those of small circles and the back ground are 17.5 and 15 respectively. The total number of detector was 100,

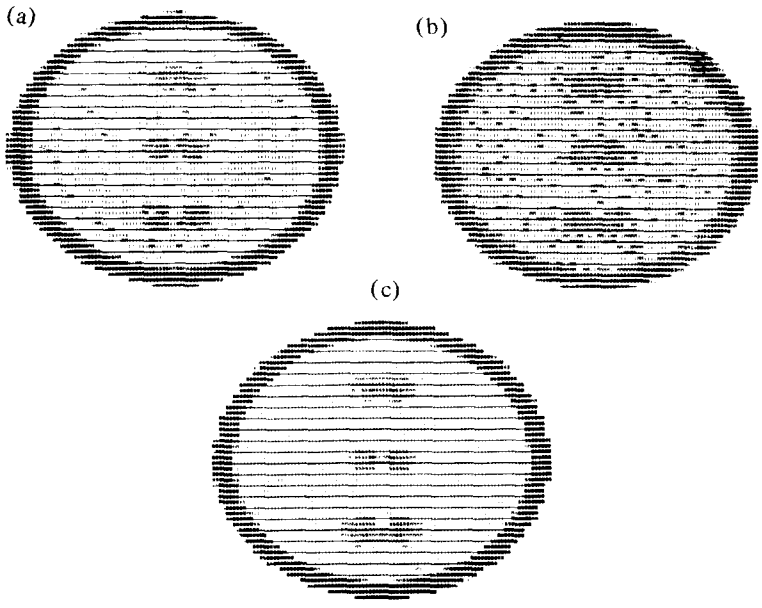

Fig. 14. Resolution Recovery in SR System.

a) Recovered image by 5 samplings per detector.
b) Blurred image by 100 detectors for noise level of 0.5%.
c) Image obtained by 500 detectors for noise level of 2.5%.

and each detector was sampled 5 times.

The motion of detector was not considered and the results are shown in Fig. 14. For the SR system case, we have made simulation only with Wiener filter method. Spatial resolution recovery was improved substantially as expected at the noise level of 0.5%. Differential method was also tested but the results were rather disappointing mainly due to the noise propagation.

IV. Conclusions

Resolution recovery was applied to the CT systems. The "Integration Blur" recovery was tried with both Wiener filter technique and differential method. The latter was so sensitive to noise that it can be concluded that the method is of little practical use. The Wiener filter approach, however, as expected, was quite successful and will be of practical use. For the direct application to CT system, both methods were applied to two CT systems, namely parallel system and stationary ring system.

In both systems, images with much improved resolution were obtained in particular with Wiener filter method. This suggests improvement of Ct image resolution without increasing the number of detectors, hence gives a low cost CT system.

We are interested in applying this resolution recovery technique, particularly the Wiener filter approach to the new PLF (Parallel Linear Fan-Beam) system which we are currently developing.[7]

Appendix: Noise Propagation

From Eq. (1-1 and Eq. (1-4),

$$g(x) = 1/T \int_{T/2}^{T/2} f(y)\, dy \qquad \text{(A-1)}$$

$$f(k) = f(k-N_d)+T\cdot(g(k-k_d)-g(k-k_d-1)) \qquad \text{(A-2)}$$

If the number of photons absorbed in one detector is p, and thus $g(k) = p \pm p^{1/2}$,

$$f(N_d+1) = f(N_d+1-N_d)+T\cdot(g(N_d+1-k_d)-g(N_d-k_d))$$
$$= p\pm T\cdot(p+(N_d-1)\cdot p/N_d)^{1/2} \qquad \text{(A-3)}$$

$$f(2N_d+1) = f(N_d+1)+T\cdot(g(2N_d+1-k_d) - g(2N_d+1-k_d-1))$$
$$= p\pm T\cdot[((2N_d-1)\cdot p/N_d)^{1/2}+((p\pm p^{1/2}) - (p\pm p^{1/2}))]$$
$$= p\pm T\cdot((2N_d-1)\cdot p/N_d+p+p)^{1/2}$$
$$= p\pm T\cdot((4N_d-1)\cdot p/N_d)^{1/2} \qquad (A\text{-}4)$$

$$f(m\cdot N_d+1) = p\pm T\cdot((2m\cdot N_d-1)\cdot p/N_d)^{1/2}$$
$$\cong p\pm T\cdot(2m)^{1/2}\cdot p^{1/2} \qquad (A\text{-}5)$$

As we can see from Eq. (A-5), noise propagates as m increases.

References

1. David Slepian, "Restoration of Photographs Blurred by Image Motion", BSTJ, pp. 2353-2362, Dec. 1967.
2. Man Mohan Sondhi, "Image Restoration: The Removal of Spatially Invariant Degradations", Proc. Vol. 60, pp. 842-853, July 1972.
3. G.N. Hounsfield, Computerized Transaxial Scanning (Tomography) part 1, Description of System, British J. of Radiology 46, 1016, 1973.
4. Z.H. Cho, General View on 3-D Image Reconstruction and Computerized Transverse Axial Tomography, Special Issue on CT, IEEE Trans. on Nucl. Sic., NS-21(3), 33, (1975).
5. Rosenfeld, "Digital Picture Processing" Academy Press, 1976.
6. Oppenheim, "Digital Signal Processing" Prentice-Hall, 1975.
7. S.Y. Lee, M.S. Thesis to be appeared.
8. M.J. Lee, M.S. Thesis of SNU, 1978.
9. Ann Souguil, et al., "A Study on the restoration of defocussed Images using Analog Filter" to be appeared.
10. ANN Souguil, Lee Myung Jong, "A Study on the Improvement of Image by TV Camera and High pass filter" 1st Convention Record on Communication Society, 1977.